Biosensors and Bioelectronics 26 (2011) 3845–3851

Contents lists available at ScienceDirect

Biosensors and Bioelectronics

journal homepage: www.elsevier.com/locate/bios

Highly stable and sensitive glucose biosensor based on covalently assembled high density Au nanostructures

Peng Si [a], Palanisamy Kannan [a], Longhua Guo [a], Hungsun Son [b], Dong-Hwan Kim [a,*]

[a] School of Chemical and Biomedical Engineering, Nanyang Technological University, 70 Nanyang Drive, Singapore 637457, Singapore
[b] School of Mechanical & Aerospace Engineering, Nanyang Technological University, Singapore 639798, Singapore

ARTICLE INFO

Article history:
Received 31 December 2010
Received in revised form 23 February 2011
Accepted 24 February 2011
Available online 3 March 2011

Key words:
Layer-by-layer
Multi-walled carbon nanotubes
Gold nanoparticles
Polyelectrolyte
Glucose oxidase
Glucose biosensor

ABSTRACT

We describe the development of a highly stable and sensitive glucose biosensor based on the nanohybrid materials derived from gold nanoparticles (AuNPs) and multi-walled carbon nanotubes (MWCNT). The biosensing platform was developed by using layer-by-layer (LBL) self-assembly of the nanohybrid materials and the enzyme glucose oxidase (GOx). A high density of AuNPs and MWCNT nanocomposite materials were constructed by alternate self assembly of thiol functionalized MWCNTs and AuNPs, followed by chemisoption of GOx. The surface morphology of multilayered AuNPs/MWCNT structure was characterized by field emission-scanning electron microscope (FE-SEM), and the surface coverage of AuNPs was investigated by cyclic voltammetry (CV), showing that 5 layers of assembly achieves the maximum particle density on electrode. The immobilization of GOx was monitored by electrochemical impedance spectroscopy (EIS). CV and amperometry methods were used to study the electrochemical oxidation of glucose at physiological pH 7.4. The Au electrode modified with five layers of AuNPs/MWCNT composites and GOx exhibited an excellent electrocatalytic activity towards oxidation of glucose, which presents a wide liner range from 20 μM to 10 mM, with a sensitivity of 19.27 μA mM^{-1} cm^{-2}. The detection limit of present modified electrode was found to be 2.3 μM (S/N = 3). In addition, the resulting biosensor showed a faster amperometric current response (within 3 s) and low apparent Michaelis–Menten constant (K_m^{app}). Our present study shows that the high density of AuNPs decorated MWCNT is a promising nanohybrid material for the construction of enzyme based electrochemical biosensors.

© 2011 Elsevier B.V. All rights reserved.

1. Introduction

Diabetes mellitus is a worldwide public disease resulting from insulin deficiency and hyperglycemia, reflected by blood glucose levels higher or lower than the normal range of 80–120 mg/dL (4.4–6.6 mM) (Wang, 2008). The complications caused by diabetes includes higher risks of heart disease, kidney failure, blindness, etc (Wang, 2001). Such complications can be greatly reduced through stringent personal control of blood glucose. The development of a highly stable and sensitive glucose biosensor is therefore of critical importance for the diagnosis and keen observation of blood glucose levels. In addition, the accurate detection of glucose is also of great interest in industrial applications such as food industry and bio-fermentation process (Wang et al., 2003). Much effort has been devoted so far on developing suitable techniques for precisely monitoring the glucose level with high sensitivity, good selectivity, high reliability and faster response.

Since the concept of enzyme electrode was first introduced by Clark and Lyons about 50 years ago (Clark and Lyons, 1962), glucose oxidase (GOx) based enzyme sensors have been widely employed to fabricate glucose biosensors. However, simple and efficient immobilization of high content of GOx on the electrode still remains a challenge for improving the performance of glucose biosensors. In the past years, a variety of nanomaterials have been widely used to structurally-modify the electrodes and immobilize GOx (Cheng et al., 2001; Deng et al., 2009; Guo and Li, 2005; Lee et al., 2008; Salimi et al., 2004; Sampath and Lev, 1996; Wang et al., 2009). Among them, gold nanoparticles (AuNPs) have drawn considerable attention because of their unique size, shape dependent physical, chemical and electronic properties when compared to the bulk gold (Daniel and Astruc, 2004; Xiao et al., 2003). It has been reported that, AuNPs can provide a suitable microenvironment, which is similar to the redox center of a native protein, to immobilize enzyme and retain their bioactivities (Zhao et al., 1992). Besides, owing to their special chemical properties, AuNPs allow a variety of functional groups, including –SH, $–NH_2$ and –CN, to bind to their surface covalently, which is favorable for the stable immobilization of biomolecules (Freeman et al., 1995; Grabar et al., 1995).

* Corresponding author. Tel.: +65 6790 4111; fax: +65 6791 1761.
E-mail address: dhkim@ntu.edu.sg (D.-H. Kim).

0956-5663/$ – see front matter © 2011 Elsevier B.V. All rights reserved.
doi:10.1016/j.bios.2011.02.044

In addition, due to their high conductivity, AuNPs can easily minimize the impedance on electrode interface and provide a necessary conduction pathway to facilitate the electron transfer between the immobilized enzyme and electrode surface (Pingarron et al., 2008). Taking account of these advantages, AuNPs were extensively used to construct glucose biosensors either alone or combined with other materials (Zhang et al., 2005a; Li et al., 2009; Ragupathy et al., 2009). However, it is difficult to attach a high density of AuNPs on the electrode surface due to the limited binding sites and low adsorption rate of AuNPs, which is not favorable for the immobilization of a large quantity of enzyme on the electrode. Consequently, the biosensor may result in low sensitivity and narrow linear range.

Layer-by-layer (LBL) is a simple and efficient method to immobilize high volume of enzyme on the electrode. Because of the simplicity of fabrication procedure, wide choice of materials and tailorable control of thickness, LBL based on electrostatic interaction has attracted tremendous interest in recent years (Chirea et al., 2007; Heath and Ratner, 2003). Wu et al. reported the amperometric glucose biosensor based on multilayered AuNPs, chitosan and GOx (Wu et al., 2007). Yan et al. fabricated a glucose biosensor via LBL self assembly of MWCNT, PDDA and GOx (Yan et al., 2007). Deng et al. constructed a glucose biosensor by assembling multilayered GOx and polyelectrolyte on MWCNTs (Deng et al., 2010). Komathi et al. proposed a glucose biosensor based on LBL assembly of MWCNT, conducting polymer, AuNPs and GOx (Komathi et al., 2009). However, the biosensors constructed via electrostatic adsorption have some major drawbacks such as instability in high ionic solution, film leaching over long time storage and long response time, which limited their application (Yan et al., 2007). While covalent binding of GOx to CNTs or AuNPs usually requires pretreatment for quite a long time with strong acid (e.g. H_2SO_4 and HNO_3) or HIO_4 (Zhang et al., 2004), which are harmful to the environment and human health. In addition, long time treatment is not favorable for industrial production. Thus, the optimal approach for the construction of glucose biosenosrs should be a mild condition which can offer both high stability and efficiency to immobilize large quantities of enzyme.

In the present study, we report a three dimensional (3-D) assembly of high density AuNPs architecture, which is constructed by LBL covalent attachment of (3-mercaptopropyl) triethoxysilane (MPTS) functionalized MWCNTs and AuNPs. This nanohybrid material can act as a suitable matrix to immobilize GOx for the fabrication of glucose biosensor. The proposed biosensor successfully overcame the problems mentioned above, which provides a stable biosensing interface, mild enzyme immobilizing environment and efficient fabrication process. MWCNTs were used in the present work to construct the 3-D structure due to their high mechanical strength, chemical stability, large surface area, and biocompatibility (Wang, 2005). In addition, MWCNTs can also facilitate the shuttling of electrons between the enzyme and the electrode surface (Agui et al., 2008). However, the poor solubility of MWCNT in most solvents is a major barrier for constructing MWCNT-based structure on electrode. In this study, MPTS was employed to covalently functionalize MWCNTs, the high density of –SH groups presented on the side walls of MWCNT not only can stabilize the MWCNT dispersion, but also provide a large amount of AuNP binding sites. The surface coverage of AuNP on electrode was found to be 90%. To the best of our knowledge, such high density of AuNPs covalently assembled on electrode surface was achieved for the first time. The resulting biosensor has achieved a remarkably enhanced sensitivity, which is much superior to multilayed GOx/MWCNT or GOx/AuNPs-based electrodes.

2. Experimental

2.1. Chemicals

Glucose, glucose oxidase from *Aspergillus niger* (GOx, 100,000–250,000 units/g), (3-Mercaptopropyl)triethoxysilane (MPTS), hydrogen tetrachloroaurate trihydrate ($HAuCl_4{\cdot}3H_2O$) and human blood serum were purchased from Sigma–Aldrich. MWCNT-COOH (OD ~50 nm, length ~20 μm, –COOH 1.23 wt%, purity 95 wt%) were obtained from Chengdu Organic Chemicals Co. Ltd., China. The human blood serum was diluted ten-fold before use. All other chemicals used in this investigation were of analytical grade and all the experimental solutions were prepared by using double distilled water.

2.2. Preparation of AuNPs and multilayered AuNPs/MWCNT electrode

AuNPs with an average diameter of ~13 nm were prepared according to the reported literature (Dubas and Schlenoff, 2001). The purification of MWCNT, preparation of multilayered AuNPs/MWCNT electrode (Wang et al., 2008; Zhang et al., 2005a) and instrumentations are discussed in supporting information.

3. Results and discussion

3.1. Characterizations of the AuNPs/MWCNT assembly

In this study, MWCNTs were first functionalized by MPTS through hydroxyl-carboxyl dehydrate reaction (Guo et al., 2010). The attached MPTS can expose large arrays of –SH groups on the end and side walls of the MWCNTs through hydrolysis, followed by self polymerization (Supplementary Scheme S1A). Then, MWCNT–Si–SH can easily adsorb on the surface of Au electrode and AuNPs through the S–H bond cleavage (Nuzzo et al., 1987). Fig. 1(A) shows one layer of MWCNTs self-assembled on the Au electrode surface through gold-thiol interaction. As can be seen the picture, the MWCNTs were uniformly distributed on the electrode surface. Afterwards, significant amount of AuNPs could easily immobilize on the end and side walls of MWCNTs via the same mechanism (Supplementary Scheme S1B). As a result, one layer of the AuNPs/MWCNT nanocomposite film was formed on the electrode surface (Fig. 1(B)). The AuNPs tethered on MWCNTs further provided the large binding sites of MWCNT–Si–SH, which allowed for the self assembly of subsequent layers. The high density of multilayered AuNPs/MWCNT nanohybrid structure was obtained on the Au electrode surface by repeating the modification process for several times. Fig. 1(C) shows the electrode modified with five layers of AuNPs/MWCNT nanocomposite architectures and depicts that the coverage of AuNPs/MWCNT on the electrode surface increased significantly compared with Fig. 1(B). In addition, the multilayered nanohybrid film shows a large surface area and high density of nanoporous structure, which allows for further immobilization of GOx and provides high accessibility toward the target molecules.

3.2. Surface coverage of AuNPs

The AuNPs coverage on the electrode surface was studied by scanning cyclic voltammograms (CV) potential range between −0.6 and 0.7 V in 0.1 M NaOH (Kumar and Zou, 2005). Fig. 2(A) shows the CVs of 1–5 layers of AuNPs/MWCNTs nanocomposite modified electrodes. The particle coverage (θ_p) is defined as the ratio between the electrochemically accessible AuNPs area and the geometric area of the Au electrode in contact with the electrolyte

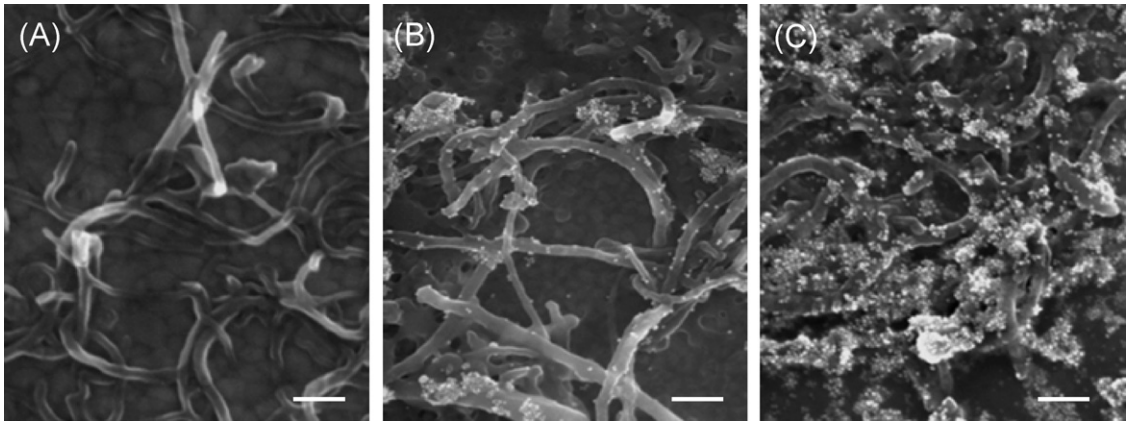

Fig. 1. FESEM images of (A) one layer of MWCNTs self assembled on Au substrate, (B) one layer of AuNPs/MWCNT nanohybrid film on Au substrate, (C) five layers of AuNPs/MWCNT modified Au substrates. The scale bar is 100 nm.

solution. The particle area was calculated by using the charge involved in the reduction of the electrochemically formed Au oxide. Assuming the charge density for the reduction of the Au oxide is 723 μC/cm^2, the particle coverage could be calculated by the following equation (Kumar and Zou, 2005; Ron and Rubinstein, 1994):

$$(\theta_p) = \frac{\text{Au oxide reduction charge}\,(\mu C)/723\,(\mu C/cm^2)}{\text{Electrode geometric area}\,(cm^2)} \times 100$$

The particle coverage of 1–5 layers of AuNPs/MWCNT modified Au electrodes were calculated to be 39%, 65%, 78%, 87% and 90% respectively. The five layered AuNPs/MWCNT nanohybrid architecture shows much superior surface particle coverage compared to the previous reports, which are 10% (Sagara et al., 2002), 25–30% (Alexeyeva and Tammeveski, 2008) and 50% (Kumar and Zou, 2005) respectively. In the present case of modification, such high surface coverage of AuNPs is achieved for the first time. Fig. 2(B) compares the surface particle coverage of the electrodes modified with 1–10 layers of the AuNPs/MWCNT nanohybrid structure. As can be seen, after 5 layers of modification of AuNPs/MWCNT layers, the surface coverage of AuNPs reached saturation point. This could be a result that when more MWCNTs assembled on the electrode, the surface area of AuNPs was increasingly covered. Thus, five layers of AuNPs/MWCNT were used throughout the experiment to modify the electrode and immobilize the enzyme.

3.3. Immobilization of GOx on multilayered AuNPs/MWCNT

The immobilization of GOx on multilayered AuNPs/MWCNT was examined by electrochemical impedance spectroscopy (EIS), which is a sensitive technique to studying the interface properties of surface modified electrodes (Ehret et al., 1997; Hall et al., 1995; Patolsky et al., 1999). It has been reported that the GOx could be chemisorbed onto the surface of AuNPs through their amino groups (Wu et al., 2007). The GOx has a three dimensional size of approximately 6 nm × 5.2 nm × 3.7 nm (Hecht et al., 1993) which could easily penetrate into the multilayered matrix of MWCNT/AuNPs nanostructure, which has the pore size of around 50 nm as observed in Fig. 1(C) and chemisorbed on the surface of AuNPs. Fig. 3 shows the typical Nyquist plot obtained for bare Au electrode, $(AuNPs/MWCNT)_5$/Au electrode and GOx/$(AuNPs/MWCNT)_5$/Au electrode. The bare Au electrode (Fig. 3(a)) presents a small semicircle followed by a linear tail. The semicircle portion illustrates an electron transfer limited process while the linear tail suggests a diffusion controlled electrochemical behavior. The diameter of the semicircle is proportional to the electron transfer resistance (R_{et}) on the electrode surface. When five layers of AuNPs/MWCNT were modified on the electrode, an increase of the impedance was observed and shown in Fig. 3(b), which was possibly caused by the electron transfer barrier formed by the bi-functional MPTS sol–gel conjugated on MWCNTs, However, the impedance was lowered by about 50% compared with monolayer of AuNPs/MWCNT modified electrode (Supplementary Fig. S2), which could contribute the good conductivity of highly assembled AuNPs. When GOx were immo-

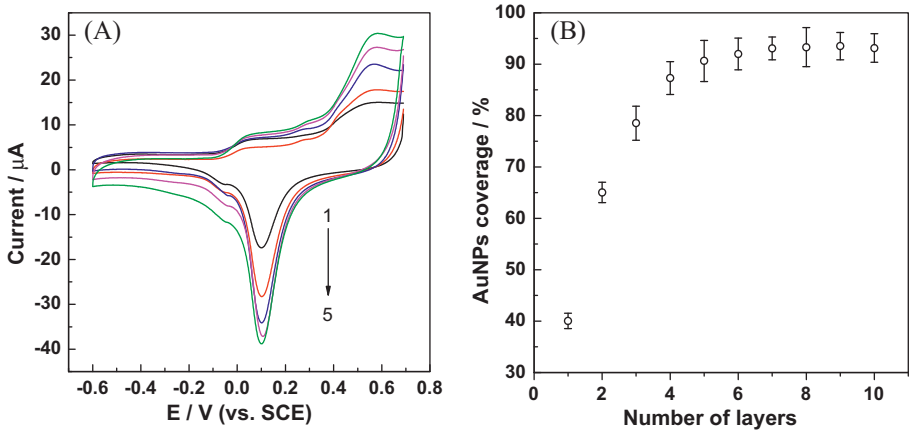

Fig. 2. (A) CVs obtained for 1–5 layers of AuNPs/MWCNT film modified Au electrode in 0.1 M NaOH. Scan rate: 50 mV/s. (B) the AuNPs coverage on Au electrode modified with 1–10 layers of MWCNT/AuNPs.

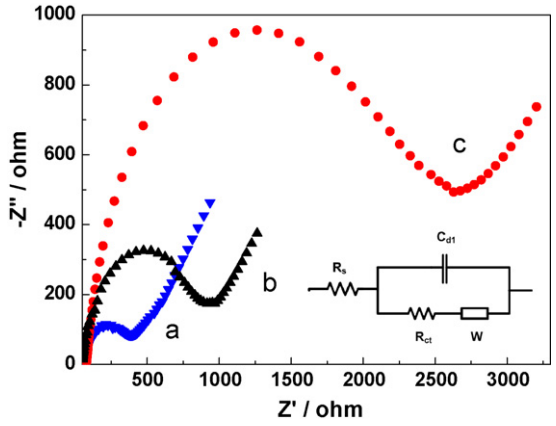

Fig. 3. Nyquist plots obtained for bare Au (a), $(AuNPs/MWCNT)_5/Au$ (b) and $GOx/(AuNPs/MWCNT)_5/Au$ electrodes (c) in 0.1 M KCl solution containing 5 mM $[Fe(CN)_6]^{4-/3-}$.

bilized on the multilayered matrix of AuNPs/MWCNT, the R_{et} was again increased by nearly four times (Fig. 3(c)). It is well known that GOx can generate an insulating layer on the electrode surface which blocked the electron transfer of $[Fe(CN)_6]^{3-/4-}$ therefore increasing the impedance of the electrode (Zhang et al., 2005b). The surface coverage of GOx (θ_E) on the electrode was calculated to be 72.4% according to the equation $\theta_E = \left(1 - R_{ct}/R_{ct}^{GOD}\right) \times 100\%$ (Liu et al., 2007), indicating the multilayered AuNPs nanostructure has the superior capability to immobilize large quantities of enzyme on the electrode surface efficiently.

3.4. Performance of the biosensors

The electrochemical behaviors of the modified electrodes were investigated by CV. Fig. 4(A) shows the cyclic voltammetric responses for 20 mM glucose recorded at GOx/MWCNT/Au, GOx/AuNPs/Au, GOx/AuNPs/MWCNT/Au and $GOx/(AuNPs/MWCNT)_5/Au$ electrodes in 0.1 M PBS (pH 7.4) containing 0.1 mM ferrocenemethanol as redox mediator. The anodic currents could be observed when the scanning potential exceeds 100 mV, which is a result of the electrocatalytic oxidation of glucose by the immobilized GOx on the multilayered film modified electrode. The oxidation of glucose can be described as the following mechanism (Bourdillon et al., 1993):

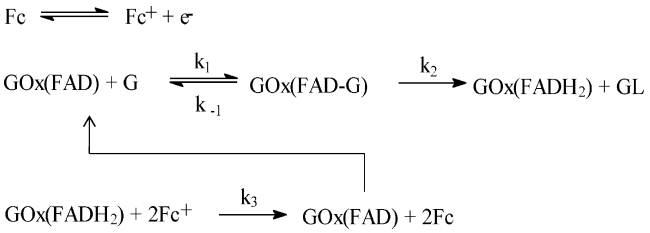

where GOx ($FADH_2$) and GOx(FAD) are the reduced and oxidized forms of GOx, Fc and Fc^+ are the reduced and oxidized forms of ferrocenemethanol (mediator), and G and GL are β-D-glucose and glucose-D-lactone, respectively.

The direct immobilization of GOx on monolayer of MWCNT or AuNPs showed poor oxidation current for glucose as can be observed in Fig. 4(A) (curves a and b). While the biosensor with GOx immobilized on one layer of AuNPs/MWCNT showed notably increased current response (Fig. 4(A) curve c), which is even higher than the summation of both a and b, indicating the GOx immobilized on AuNPs/MWCNT nanohybrid has much superior electrocatalytic activity towards the oxidation of glucose. The result is consistent with the previous report in which the electrode was modified with Pt nanoparticles and MWCNT (Yang et al., 2006a). Surprisingly, the Au electrode modified with 5 layers of AuNPs/MWCNT and GOx showed an enhanced oxidation current response of 21.5 mA, which is more than five times higher than the single layer hybrid modified electrode (Fig. 4(A) d). The observed result indicates that the multilayered construction of AuNPs/MWCNT significantly improved the sensitivity of the glucose biosensor, which might contribute to the increases the both surface area and the enzyme loading capability of the electrode. As can be seen in Fig. 4(A) inset, the bare Au electrode (dashed curve) displayed a couple of poor redox peaks at the scan rate of 50 mV/s in 0.1 M PBS. After modification with 5 layers of AuNPs/MWCNT and GOx, notably enhanced redox peak current was observed and shifted towards the less positive potential side (solid curve), indicating that favorable electron transfer behavior of the multilayered AuNPs/MWCNT nanohybrid materials. The current response of the resulting glucose biosensor modified with 1–10 layers of AuNPs/MWCNT and GOx for 20 mM glucose are compared in Fig. 4(B). We found that the current response rises with the increase of first five layers of AuNPs/MWCNT on the electrode surface, while a plateau current was observed from the sixth layer. This result suggest that the surface coverage of AuNPs, implying that AuNPs plays

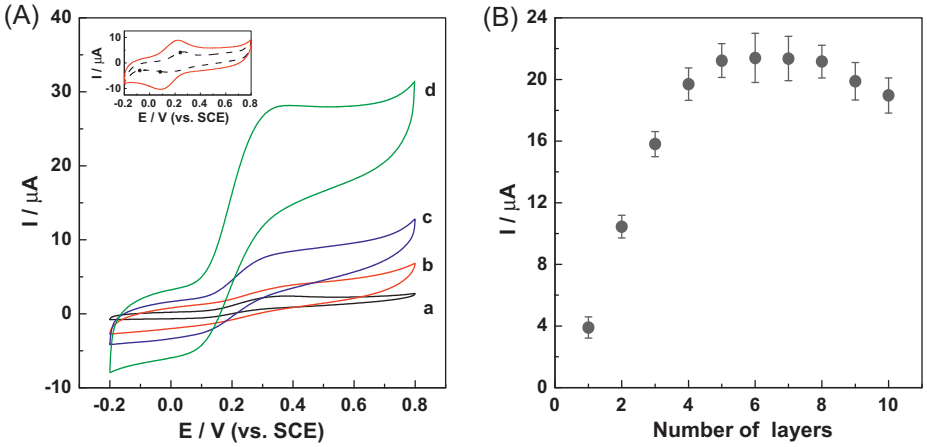

Fig. 4. (A) CVs response of GOx/AuNPs/Au (a), GOx/MWCNT/Au (b), GOx/AuNPs/MWCNT/Au (c) and $GOx/(AuNPs/MWCNT)_5/Au$ electrodes (d) in 0.1 M PBS containing 0.1 mM ferrocenemethanol and 20 mM glucose. Inset: CVs response of bare Au (dashed) and $GOx/(AuNPs/MWCNT)_5/Au$ electrodes (solid) in 0.1 M PBS containing 0.1 mM ferrocenemethanol. (B) The current response for 20 mM glucose on Au electrode modified with 1–10 layers of AuNPs/MWCNT and GOx. The scan rate is 50 mV/s.

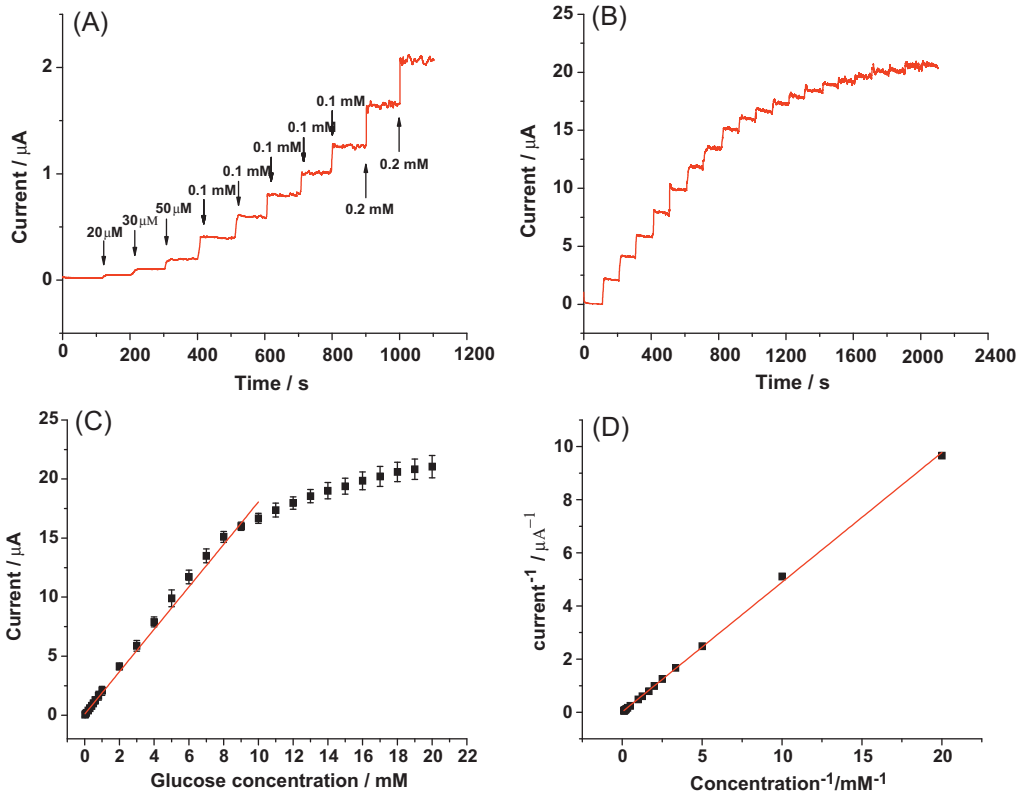

Fig. 5. (A) Amperometric response of the GOx/(AuNPs/MWCNT)$_5$/Au electrode to successive addition of different concentrations of glucose at applied potential of 0.3 V (vs. SCE) in PBS containing 0.1 mM ferrocenemethanol. (B) Amperometric response of the above electrode to successive addition of 1 mM glucose at applied potential of 0.3 V (vs. SCE) in PBS containing 0.1 mM ferrocenemethanol. (C) The calibration curve of present glucose biosensor obtained from (A) and (B). (D) Lineweaver–Burk plot obtained for the above glucose biosensor for the determination of K_m^{app}.

an essential role for the immobilization of GOx. Finally, the decreasing current response was observed after the eighth layer. This could result from the diffusion blockage of target molecules and mediators on the electrode surface for high density of MWCNT structure would make the electrode less porous and inaccessible to the small molecules of analytes.

Supplementary Fig. S3(A) shows the CVs of the GOx/(AuNPs/MWCNT)$_5$/Au electrode in PBS containing 0 1 mM ferrocenemethanol at different scan rates. Both anodic and cathodic peak currents were linear against the square root of the scan rates ranging from 20 to 300 mV/s and the corresponding calibration plot is shown in Supplementary Fig. S3(B). This result illustrates that the electrochemical process on the electrode surface was diffusion controlled and the self assembled nanostructure multilayer on the electrode was highly accessible to the redox mediator.

3.5. Amperometric sensing of glucose

Amperometric method was used to examine the sensitivity of the resulting GOx/(AuNPs/MWCNT)$_5$/Au electrode towards the detection of glucose. Fig. 5(A) shows the amperometric i–t curve response of the present glucose biosensor upon the successive addition of different concentrations of glucose in a homogeneously stirred PBS (pH 7.4) at a constant applied potential of 0.3 V (vs. SCE) until the glucose level in the solution reached up to 1 mM. The resulting biosensor exhibited rapid and sensitive responses to the addition of glucose, which reached 95% of the steady state current within 3 s. Two aspects might contribute to the fast response. First, the highly porous nanostructure of multilayered AuNPs/MWCNT allows rapidly, the diffusion of glucose and mediator from bulk solution to the enzyme. Second, the highly assembled AuNPs yields a good conduction pathway, which facilitates the electron transfer between the mediator and the electrode surface. Fig. 5(B) shows the amperogram of the GOx/(AuNPs/MWCNT)$_5$/Au electrode upon the successive addition of 1 mM glucose operating at the same experimental conditions as in Fig. 5(A). When the glucose reached a high concentration, a plateau current can be observed, showing the typical characteristic features of Michaelis–Menten kinetics (Kopelman, 1988). The calibration plot (Fig. 5(C)) obtained from amperometry results (Fig. 5(A) and (B)), shows that the present glucose biosensor has a wide linear range from 20 μM to 10 mM, with a sensitivity of $19.27 \pm 0.5\ \mu A\ mM^{-1}\ cm^{-2}$ and the detection limit of 2.3 μM (S/N = 3). The sensitivity of the present electrode is approximate three times higher than multilayered GOx/AuNPs modified electrode (Yang et al., 2006b) and two times higher than multilayed GOx/MWCNTs-based electrode (Yan et al., 2007).

The apparent Michaelis–Menten constant was calculated from the electrochemical version of the Lineweaver–Burk plot (Lineweaver and Burk, 1934):

$$\frac{1}{i_{ss}} = \frac{K_m^{app}}{i_{max}}\frac{1}{C} + \frac{1}{i_{max}}$$

where i_{ss} is the steady-state current after addition of glucose, i_{max} is the maximum current measured under saturated substrate condition and C is the bulk concentration of the substrate. The K_m^{app} was determined by analysis of the slope and intercept of the double-reciprocal plot of the steady-state current vs. glucose concentration as shown in Fig. 5(D). The K_m^{app} was calculated to be 6.7 mM, which is much smaller than previously reported values in the literatures (10.5 mM (Wu et al., 2007), 14.9 mM (Ozoemena and Nyokong, 2006) and 20 mM (Sampath and Lev, 1996) respectively). The smaller K_m^{app} value means that the immobilized GOx

Table 1
Determination of glucose in human blood serum sample using GOx/(AuNPs/MWCNT)$_5$/Au electrode.

Sample	Found (mM)	Added (mM)	Found (mM)	R.S.D. (%)	Recovery (%)
1	3.52	2.00	5. 63	4.2	102
2	3.52	4.00	7.89	2.9	105
3	3.52	6.00	9.14	3.7	96

well retained their electrocatalytic activity and the biosensor has strong affinity towards the analyte glucose.

3.6. Studies of interferences and stability

We have also studied the determination of glucose in the presence of common physiological interferents such as ascorbic acid (AA), uric acid (UA) and acetaminophen (AP) by amperometric method. Supplementary Fig. S4 shows the amperometric *i*–*t* curve responses of the GOx/(AuNPs/MWCNT)$_5$/Au electrode for 0.5 mM of AA, 0.5 mM AP, 1 mM UA and 0.5 mM glucose in a homogeneously stirred 0.1 M PBS (pH 7.4) at a constant applied potential of 0.30 V. The initial addition of 0.5 mM each AA, AP and 1 mM UA with a sample interval of 100 s into the homogeneously stirred PBS yields an insignificant change of amperometric current, while the addition of 0.5 mM glucose evoked the rapid response of higher ampmetric current. The current responses of the interferents are negligible compared to that induced by the glucose, indicating the present glucose biosensor is feasible for the determination of glucose in the presence of common interfering compounds.

The operating stability of our five layers of AuNPs/MWCNT nanocomposite electrode toward the voltammetric detection has been evaluated. The voltammetric oxidation current was tested by potential cycling from −0.2 to 0.8 V in the presence of 10 mM glucose at a scan rate of 50 mV/s. No obvious anodic current decrease was observed during 30 cycles of measurement. The storage stability was examined by measuring the amperometric response of the resulting biosensor to 10 mM glucose everyday and keeping the modified electrode at 4 °C in 0.1 M PBS after use. The biosensor remained 95.4% of its initial current intensity after one week (Supplementary Fig. S5). The long-term storage stability reflects the excellent durability of the self-assembled multilayer films and good biocompatibility of the multilayered AuNPs/MWCNT matrix toward immobilizing GOx.

3.7. Determination of glucose in human blood serum

The GOx/(AuNPs/MWCNT)$_5$/Au electrode was further employed to detect glucose levels in healthy human blood serum sample by using the calibration curve obtained above. The original glucose concentration in the serum was determined to be 3.52 mM, the corresponding results after addition of standard glucose solution were listed in Table 1. A small relative standard deviation (R.S.D) value (less than 4.2%) was obtained from 6 parallel modified electrodes, indicating that the good reproducibility of the present fabrication method, while high recovery values (96–102%) showed the capability of the biosensor for real sample detection. These results demonstrate that the proposed biosensor is reliable and effective.

4. Conclusions

In summary, we successfully fabricated a glucose biosensor by immobilizing large quantities of GOx on a high density AuNPs matrix, which composed of multilayered AuNPs/MWCNT nanohybrid structure. A high surface coverage of AuNPs was achieved by the multilayered AuNPs/MWCNT nanohybrid architecture, which effectively facilitated the electron transfer, lowered the charge transfer resistance and enhanced the enzyme loading capability of the electrode. The covalent assembly of multilayered AuNPs and MWCNT provides a highly stable biosensing interface which effectively improves the durability of the electrode for long time storage. The five layers of AuNPs/MWCNT composites and GOx exhibited an excellent electrocatalytic activity towards oxidation of glucose, which presents a wide liner range from 20 μM to 10 mM, with a sensitivity of 19.27 μA mM^{-1} cm^{-2} and a detection limit of 2.3 μM (S/N = 3). The resulting glucose biosensor (GOx/(AuNPs/MWCNT)5/Au electrode) showed much superior sensitivity than the multilayered GOx/MWCNT- or multilayered GOx/AuNPs-based electrodes. In addition, the proposed biosensor electrode exhibited satisfied recovery results when employed to determine glucose levels in human blood serum sample. The many advantages of multilayered AuNPs/MWCNT nanostructure reported in our present study can provide great potentials for development of other enzyme-based biosensors.

Acknowledgments

We gratefully acknowledge the Nanyang Technological University for support of this work. We also thank financial support from the Academic Research Funding Tier 1 (RG65/08) and the National Medical Research Council (NMRC/NIG/00602009) of Singapore.

Appendix A. Supplementary data

Supplementary data associated with this article can be found, in the online version, at doi:10.1016/j.bios.2011.02.044.

References

Agui, L., Yanez-Sedeno, P., Pingarron, J.M., 2008. Anal. Chim. Acta 622, 11–47.
Alexeyeva, N., Tammeveski, K., 2008. Anal. Chim. Acta 618, 140–146.
Bourdillon, C., Demaille, C., Gueris, J., Moiroux, J., Saveant, J.M., 1993. J. Am. Chem. Soc. 115, 12264–12269.
Cheng, Z., Wang, E., Yang, X., 2001. Biosens. Bioelectron. 16, 179–185.
Chirea, M., Pereira, C., Silva, F., 2007. J. Phys. Chem. C 111, 9255–9266.
Clark, L.C., Lyons, C., 1962. Ann. N.Y. Acad. Sci. 102, 29–45.
Daniel, M.-C., Astruc, D., 2004. Chem. Rev. 104, 293–346.
Deng, S., Jian, G., Lei, J., Hu, Z., Ju, H., 2009. Biosens. Bioelectron. 25, 373–377.
Deng, C., Chen, J., Nie, Z., Si, S., 2010. Biosens. Bioelectron. 26, 213–219.
Dubas, S.T., Schlenoff, J.B., 2001. Langmuir 17, 7725–7727.
Freeman, R.G., Grabar, K.C., Allison, K.J., Davis, J.A., Guthrie, A.P., Hommer, M.B., Jackson, M.A., Smith, P.C., Walter, D.G., Natan, M.J., 1995. Science 267, 1629–1632.
Grabar, K.C., Freeman, R.G., Hommer, M.P., Natan, M.J., 1995. Anal. Chem. 67, 735–743.
Guo, D.J., Li, H.L., 2005. Carbon 43, 1259–1264.
Guo, L., Chen, G., Kim, D.H., 2010. Anal. Chem. 82, 5147–5153.
Hall, E.A.H., Skinner, N.G., Jung, C., Szunerits, S., 1995. Electroanalysis 7, 830–837.
Heath, J.R., Ratner, M.A., 2003. Phys. Today 56, 43–49.
Hecht, H.J., Kalisz, H.M., Hendle, J., Schmid, R.D., Schomburg, D., 1993. J. Mol. Biol. 229, 153–172.
Komathi, S., Gopalan, A.I., Lee, K.-P., 2009. Biosens. Bioelectron. 24, 3131–3134.
Kopelman, R., 1988. Science 241, 1620–1626.
Kumar, S., Zou, S., 2005. J. Phys. Chem. B 109, 15707–15713.
Lee, S.-R., Lee, T.-Y., Sawada, K., Takao, H., Ishida, M., 2008. Biosens. Bioelectron. 24, 410–414.
Li, F., Wang, Z., Shan, C., Song, J., Han, D., Niu, L., 2009. Biosens. Bioelectron. 24, 1765–1770.
Lineweaver, H., Burk, D., 1934. J. Am. Chem. Soc. 56, 658–666.
Liu, H., Tian, Y., Deng, Z., 2007. Langmuir 23, 9487–9494.
Nuzzo, R.G., Zegarski, B.R., Dubois, L.H., 1987. J. Am. Chem. Soc. 109, 733–740.
Ozoemena, K.I., Nyokong, T., 2006. Electrochim. Acta 51, 2669–2677.
Patolsky, F., Zayats, M., Katz, E., Willner, I., 1999. Anal. Chem. 71, 3171–3180.
Pingarron, J.M., Yanez-Sedeno, P., Gonzalez-Cortes, A., 2008. Electrochim. Acta 53, 5848–5866.

Ragupathy, D., Gopalan, A.I., Lee, K.-P., 2009. Electrochem. Commun. 11, 397–401.
Ron, H., Rubinstein, I., 1994. Langmuir 10, 4566–4573.
Sagara, T., Kato, N., Nakashima, N., 2002. J. Phys. Chem. B 106, 1205–1212.
Salimi, A., Compton, R.G., Hallaj, R., 2004. Anal. Biochem. 333, 49–56.
Sampath, S., Lev, O., 1996. Anal. Chem. 68, 2015–2021.
Wang, J., 2001. Electroanalysis 13, 983–988.
Wang, J., 2005. Electroanalysis 17, 7–14.
Wang, J., 2008. Chem. Rev. 108, 814–825.
Wang, S.G., Zhang, Q., Wang, R., Yoon, S.F., Ahn, J., Yang, D.J., Tian, J.Z., Li, J.Q., Zhou, Q., 2003. Electrochem. Commun. 5, 800–803.
Wang, J., Liu, G., Lin, Y., 2008. Biomol. Catal., 117–128, Chpt. 6.
Wang, Z., Liu, S., Wu, P., Cai, C., 2009. Anal. Chem. 81, 1638–1645.
Wu, B.-Y., Hou, S.-H., Yin, F., Li, J., Zhao, Z.-X., Huang, J.-D., Chen, Q., 2007. Biosens. Bioelectron. 22, 838–844.
Xiao, Y., Patolsky, F., Katz, E., Hainfeld, J.F., Willner, I., 2003. Science 299, 1877–1881.
Yan, X.B., Chen, X.J., Tay, B.K., Khor, K.A., 2007. Electrochem. Commun. 9, 1269–1275.
Yang, M., Yang, Y., Yang, H., Shen, G., Yu, R., 2006a. Biomaterials 27, 246–255.
Yang, W., Wang, J., Zhao, S., Sun, Y., Sun, C., 2006b. Electrochem. Commun. 8, 665–672.
Zhang, S., Yang, W., Niu, Y., Sun, C., 2004. Sens. Actuators B 101, 387–393.
Zhang, S., Wang, N., Niu, Y., Sun, C., 2005a. Sens. Actuators B 109, 367–374.
Zhang, S., Wang, N., Yu, H., Niu, Y., Sun, C., 2005b. Bioelectrochemistry 67, 15–22.
Zhao, J., Henkens, R.W., Stonehuerner, J., O'Daly, J.P., Crumbliss, A.L., 1992. J. Electroanal. Chem 327, 109–119.